Research Square

Preprints are preliminary reports that have not undergone peer review.
They should not be considered conclusive, used to inform clinical practice,
or referenced by the media as validated information.

South America's extinct notoungulates evolved a masticatory system with no living analogue

José-Ignacio Arriagada Díaz

joseignacioarriagadadiaz@gmail.com

Austral University of Chile

Karen Moreno

Austral University of Chile

Marcos Fernández-Monescillo

Universidad Complutense de Madrid

Kornelius Kupczik

University of Chile

Article

Keywords: Notoungulata, functional morphology, masticatory biomechanics, non- analogues

Posted Date: November 11th, 2026

DOI: https://doi.org/10.21203/rs.3.rs-11460944/v1

License: This work is licensed under a Creative Commons Attribution 4.0 International License.
Read Full License

Additional Declarations: No competing interests reported.

South America's extinct notoungulates evolved a masticatory system with no living analogue.

José-Ignacio Arriagada Díaz [1-2*], Karen Moreno[1*], Marcos Fernández-Monescillo[3,4,5], Kornelius Kupczik[6]

[1] Universidad Austral de Chile, Instituto de Ciencias de la Tierra, Universidad Austral de Chile, Valdivia.
[2] Escuela de Medicina Veterinaria, Facultad de Recursos Naturales y Medicina Veterinaria, Universidad Santo Tomás, Viña del Mar, Chile
[3] Departamento de Geodinámica, Estratigrafía y Paleontología (GEODESPAL), Facultad Ciencias Geológicas, Universidad Complutense de Madrid, 28040 Madrid, Spain.
[4] Consejo Nacional de Investigaciones Científicas y Técnicas (CONICET), Godoy Cruz 2290, C1425FQB, Ciudad Autónoma de Buenos Aires, Argentina.
[5] Museo de Paleontología, Facultad de Ciencias Exactas, Físicas y Naturales, Universidad Nacional de Córdoba, Vélez Sarsfield 1611, (X5016GCA) Córdoba, Argentina.
[6] Departamento de Antropología, Facultad de Ciencias Sociales, Universidad de Chile, Santiago de Chile.

Corresponding authors E-mails: joseignacioarriagadadiaz@gmail.com; karenmoreno@uach.cl

Contributing authors: marcfe24@ucm.es; kornelius.kupczik@uchile.cl

Abstract

Reconstructing how extinct mammals fed rests on a uniformitarian assumption: that their anatomy has a functional counterpart among living species. Notoungulata, a diverse clade of extinct South American herbivorous mammals that evolved across a wide range of ecological niches during nearly 60 Myr of South American isolation, challenges this assumption. They have been likened to rodents, lagomorphs, ungulates, hyraxes, rhinoceroses, and wombats, yet each comparison captures only part of their anatomy, and none provides a complete functional match. Whether this reflects incomplete analogy or genuine functional novelty remains unresolved. We tested all proposed feeding analogues within a single integrated framework, combining geometric morphometrics, temporomandibular joint (TMJ) indices, lever mechanics and finite element analysis across 12 notoungulates (four families, Oligocene–Pleistocene) and 128 extant herbivorous and omnivorous mammals. No living group reproduced the notoungulate masticatory system. Instead, each component matched a different analogue: mandibular shape approached hyraxes and rhinoceroses, TMJ architecture suids and tapirs, molar lever mechanics ungulates, and incisor-bite stress the most resistant rodents. Integrated in a short, robust mandible with a fused symphysis, this mosaic yielded the lowest incisor-bite stresses of all sampled clades and molar-bite stresses below those of most ungulates and diprotodontians. Notoungulates formed a cohesive functional cluster distinct from extant herbivores, with disparity concentrated in typotheres and culminating in the highly mobile jaw of *Pachyrukhos*. Prolonged isolation thus produced a novel solution to herbivory rather than convergence on modern designs, showing that analogue-based reconstructions can mask functional innovation in extinct endemic radiations.

Keywords: Notoungulata, functional morphology, masticatory biomechanics, non- analogues.

1 Introduction

Inferring feeding behaviour in extinct mammals typically relies on comparisons with extant taxa linking morphology, biomechanics, and ecology. However, this framework becomes uncertain when novel anatomical features limit comparisons with modern analogues [1]. This is especially true for Notoungulata, a mammalian order that diversified across a wide range of ecological niches during nearly 60 Myr of South American isolation, before becoming extinct in the early Holocene (~10 ka), well after the Great American Interchange (~3 Ma) [2–4]. From the Oligocene onwards, the order was dominated by two major clades: the large–bodied Toxodontia and the generally smaller Typotheria, traditionally comprising the families Mesotheriidae, Interatheriidae and Hegetotheriidae [5–7].

Their cranial synapomorphies are primarily expressed in the temporal region of the skull and in a suite of distinctive dental traits [2, 8–11]. Notoungulate dentition was highly diverse, with brachydont, hypsodont, and even hypselodont cheek teeth evolving independently across lineages. The recurrent acquisition of hypsodonty, followed in some clades by the evolution of rootless, ever-growing dentition, has been linked to climatic aridification and increased dental wear driven by abrasive diets, including silica-rich grasses, or incidental ingestion of volcanic ash and exogenous grit [12–16]. Yet, dietary interpretations often conflict, with notoungulate lineages variously reconstructed as grazers, browsers, mixed feeder, or hard item consumer, including fruits and seeds [17–26]

Despite broad agreement that notoungulates were herbivorous, their masticatory biomechanics remain contentious. In toxodontids, well-developed temporalis musculature has been

interpreted as indicating a relatively plesiomorphic mammalian masticatory pattern dominated by ventrodorsal movement, a condition shared by most notoungulates [18, 27], whereas their exceptionally developed pterygoid and masseter musculature has been regarded as evidence for an ungulate–like grinding mechanism characterized by predominantly sub–horizontal jaw movements, rather than extensive transverse motion [14, 27, 28]. Some typotheres, particularly mesotheriids and *Pachyrukhos*, have been proposed to exhibit a rodent–like gnawing masticatory pattern owing to the more anterodorsal origin of the masseter on the zygomatic plate [18, 29].

Mandibular morphology likewise departs markedly from that of most extant herbivores. Rather than the elongate, gracile mandibles typical of grazing ungulates (30), notoungulates generally possessed short, robust mandibular bodies, extensive symphyseal fusion and a reduced or absent diastema [9, 19, 31]. Temporomandibular joint morphology also varies substantially across the order, from lateromedially expanded to oval or sinusoidal mandibular condyles [18, 20, 21], suggesting distinct patterns of jaw kinematics. However, how these components interact to generate bite forces and jaw movements remains poorly understood.

Perhaps the clearest indication of this uncertainty is the remarkable breadth of extant analogues proposed for notoungulates. Thus, toxodontids have been compared to rhinoceroses based on their massive skulls, hypsodont dentitions, and dental wear patterns [31, 32]; to hippopotamuses because of their inferred use of riverine habitats [33]; and giraffes in terms of dietary niche [22]. Typotheres, in turn, have been proposed as analogues of rodents owing to their procumbent incisors, hypsodonty, and inferred masticatory movements [2, 3, 16, 18]; lagomorphs because of their overall cranial proportions and masseteric configuration [3, 29]; ungulates based on mesowear and inferred grinding movements [28]; tapirs, hyraxes, and rhinoceroses based on cranial and mandibular morphology [31]; and wombats because of masseter insertion and digging capabilities [13, 29, 34].

Beyond these multiples analogies —useful for capturing broad ecological and functional similarities— lies the possibility that notoungulates evolved an independent mosaic of functional traits rather than converging on any extant herbivore. Were notoungulates simply ecological analogues of modern herbivores, or did prolonged isolation in South America produce a novel morphofunctional solution to herbivory?

Mandibular and temporomandibular joint morphology are pivotal determinants of bite force transmission and masticatory kinematics, making them powerful proxies for reconstructing feeding function in extinct mammals [12, 35]. Using geometric morphometrics, biomechanical lever models and finite element analyses, we test all major previously proposed extant analogues within a single integrated framework, assessing how mandibular morphology influences biomechanical performance across Oligocene to Pleistocene representatives of Typotheria and Toxodontia. Specifically, we ask whether notoungulates occupied the morphofunctional space of living herbivores or evolved a novel biomechanical solution, expanding the known range of mammalian feeding adaptations.

2 Results

2.1 Mandibular shape

The first principal component (PC1) explains 56.13% of total shape variation and primarily reflects changes in mandibular body length and thickness, together with anterior–posterior displacement of the coronoid process (Fig. 1). Negative PC1 scores correspond to an ungulate-like morphology, characterized by an elongated, slender mandibular body and tooth row,

elongated diastema, dorsally elevated coronoid process, and forward–facing incisors. Bovidae, Cervidae, Tragulidae, Camelidae, Giraffidae and Equidae occupy this end of the axis. Positive scores are restricted to rodents (Sciuromorpha, Myomorpha and Hystricomorpha), characterized by shorter, more robust mandibles, lower and more anteriorly positioned ramus, and upward-facing procumbent incisors. Except for the typotheriid interatheriid *Miocochilius anomopodus* and hegetotheriid *Pachyrukhos moyani*, Notoungulata occupy an intermediate position between ungulates and rodents (relative landmark shifts along PC1 and PC2 are shown in Supplementary Fig. S1 online). Whereas toxodontids and mesotheriid typotheres occupy a relatively conserved region of morphospace near zero, interatheriid and hegetotheriid typotheres show greater variation, extending slightly towards both negative and positive scores.

The second principal component (PC2) accounts for 10.78% of total shape variation and primarily reflects differences in gonion shape and mandibular corpus curvature (Fig. 1). Positive scores correspond to a relatively straight corpus, a marked angular process and incisors protruding beyond the post-canine cheek teeth, whereas negative scores indicate a dorsoventrally flexed corpus, expanded gonial angle without an angular process, anteriorly facing condyle and incisors positioned at the level of the post-canine tooth row. Most extant taxa overlap around zero, whereas Notoungulata, except for *M. anomopodus* and *P. moyani*, occupy the negative region, particularly mesotheriid typotheres. The third principal component (PC3) accounts for an additional 8.23% of total shape variation; associated shape changes are described and shown in supplementary Fig. S2 online.

Allometry explained 34.5% of shape variation ($p < 0.0001$; see Supplementary Fig. S3 online). Size-corrected PCA (PC1–2: 54.2% of variation) showed greater overlap among taxa while retaining the main morphological gradient from derived ungulate morphology at negative PC1 scores to rodents at the positive end. Relative to the uncorrected PCA, Suidae, Tapiridae and Notoungulata shifted towards more positive PC1 scores. Interatheriidae and Hegetotheriidae clustered closer to zero, overlapping with Sciuromorpha, whereas Toxodontidae shifted further towards the positive end. Mesotheriidae remained distinct, combining a short, robust mandibular body with a tall ramus (see Supplementary Fig. S4 online). In both PCAs, *Ceratotherium simum* and *Heterohyrax brucei* were the only extant taxa plotting closest to Notoungulata.

2.2 Temporomandibular joint morphology

The non-hierarchical clustering revealed that CI and GCI are distributed diagonally from the lower–left to the upper–right corner of morphospace, primarily contributing to Dim 1 (x-axis), which explains 83% of the total variance (Fig. 2). Both indices are highly correlated ($r = 0.91$, $p < 0.01$; see Supplementary Fig. S5 online). Along this axis, Notoungulata clusters with Ungulata (cluster 3), characterized by lateromedially expanded joints and a strong correspondence between CI and GCI (negative values). Most rodents fall into two distinct clusters (1 and 2), except for a few sciuromorphs (see below). Cluster 1 comprises taxa with more anteroposteriorly elongated joints (CI and GCI values 1–2), whereas cluster 2 is characterized by relatively rounded condyles and glenoid cavities (CI and GCI values 0–1). Cluster 2 also exhibits greater condyle–glenoid decoupling than clusters 1 and 3. Likewise, marsupials fall in cluster 3, except for macropodids, which are positioned closer to rodents owing to their relatively rounded joint morphology (see Supplementary Figs. S6–S7 online).

Dim 2 (y-axis) explains 14.2% of the variance (Fig. 2) and primarily reflects variation in condylar curvature. All taxa in cluster 3 are distributed along this axis according to condylar curvature, with Notoungulata occupying the negative end together with Suidae, Tapiridae,

Wombatidae, and a few sciuromorph rodents (Casfib, Cascan, Cynlud, and Bislao), all characterized by convex condyles. In contrast, Bovidae, Cervidae, Tragulidae, and Giraffidae occupy the positive end, characterized by flatter condyles (see Supplementary Figs. S6–S8 online). Within Notoungulata, toxodontids and mesotheriid typotheres exhibit similar values across all three indices, with lateromedially expanded joints and slightly flatter condyles than interatheriid and hegetotheriid typotheres, which retain comparatively rounded condyles. *Pachyrukhos* (Pacmoy) is the most distinctive notoungulate, exhibiting the greatest condyle–glenoid decoupling. A similar but less pronounced pattern occurs in Interatheriidae, whereas the remaining notoungulates show closer correspondence between the two articular surfaces (see Supplementary Fig. S5 online).

2.3 Mechanical advantage

Along the four bite point positions tested, MA values exhibited a significant correlation (see Supplementary Fig. S5 online). However, BP1 and BP4 showed a reduction of linearity ($R2 = 0.76$; $p < 0.05$) compared to BP1 vs BP2-3 ($R2 = 0.8$, 0.9 respectively). Given their lower predictive power, we retained BP1 and BP4 for cross-taxon comparisons because they represent functionally distinct bite types (incisor and molar bites) spanning the full anteroposterior range of masticatory function across taxa.

2.3.1 Anterior most incisor bite (BP1)

Except for Tragulidae, artiodactyls exhibit a lower median masseter MA below 25%, whereas the perissodactyls show intermediate values ranging from 27% to 35% (Fig. 3). Higher median values (MA> 35%) are characteristic of Hystricomorpha, Myomorpha, Sciuromorpha, and Wombatidae. Notoungulata exhibits a masseter MA value between 25 and 35%, overlapping with the range observed in Perissodactyla, Leporidae and Diprotodontia. However, considerable variation is present within the order toxodontids exhibit the lowest MA values (22% to 26%), followed by interatheriids (26% to 31%) and the hegetotheriid *Hegetotherium* (28%). Mesotheriids consistently show relatively high MA values (31% to 33%), exceeded only by the hegetotheriid *Pachyrukhos*, the only notoungulate reaching the upper end of the distribution (38% MA).

Temporalis MA ranges between 5 and 15% in nearly all taxa, with the notable exception of Leporidae (4%) and Diprotodontia (16%). Within Notoungulata, hegetotheriids exhibit the lowest temporalis MA values (6%), whereas the remaining families lie close to the upper limit of the range at 14% (Fig. 3) clearly exceeding the mean values recorded for most artiodactyls and rodents. Interestingly, *Tapirus* and *Ceratotherium* overlap Notoungulata.

2.3.2 Posterior most molar bite (BP4)

Modern ungulates typically exhibit masseter MAs between 60% and 90%, except for Tragulidae and Suidae (Fig. 4). In contrast, Hyracoidea, Miomorpha, Sciuromorpha, and Wombatidae possess masseter MA near or exceeding 100%. Notoungulates share masseter MA values with the modern ungulates, Leporidae, and Diprotodontia, falling within a range of 58% to 80%. Specifically, Toxodontidae exhibits the lowest values within the order (55% to 62%), Mesotheriidae occupies the intermediate range (64% to 66%), whereas the typotheres Hegetotheriidae and Interatheriidae display the highest values (71% to 81%).

The temporalis MAs at the posterior most molar bite point (BP4) follow a pattern like that observed at BP1 (Fig. 4), showing considerable overlap among extant and fossil taxa.

Hegetotheriidae presents the lowest temporalis MA value among notoungulates (18%), while the remaining families exhibit higher mechanical efficiencies, reaching a mean value of 30%.

2.4 Finite element analysis

2.4.1 Load case: Anterior most incisor bite

Notoungulata shows the lowest mean stress values, ranging from 0.38 to 1.48 MPa (Fig. 5). Within the order, mesotheriids generally show the lowest values (0.44–0.60 MPa), followed by toxodontids and interatheriids (0.56–0.90 MPa). *Interatherium robustum* shows the lowest mean stress among notoungulates (0.38 MPa), whereas *Hegetotherium mirabile* shows the highest (1.48 MPa). *Pachyrukhos moyani* falls within the toxodontid–interatheriid range (0.69 MPa).

Most ungulates and Diprotodontia show higher mean stress values than Notoungulata. *Giraffa camelopardalis* shows the highest value across the dataset (Gircam: 4.24 MPa). Conversely, Suidae (Babbab: 0.69–Potpor: 1.59 MPa) and Perissodactyla (Tapkab: 1.20–Equfer: 1.51 MPa) show lower values than most artiodactyls, with *Babyroussa* and *Tapirus* overlapping the upper notoungulate range.

Among non-ungulates, the procaviid *Heterohyrax brucei* falls within the mesotheriid range (Hetbru: 0.66 MPa). Rodentia spans a broader range (Hystricomorpha: Ctebid: 0.51–Cavape: 2.46 MPa; Myomorpha: Olinig: 0.78–Musmus: 2.84 MPa; Sciuromorpha: Gueing: 0.69–Specit: 2.09 MPa). However, only some genera overlap the notoungulate range (asterisks in Fig. 5): *Ctenomys*, *Heterocephalus* and *Trinomys* (Hystricomorpha); *Holochilus* and *Oligoryzomys* (Myomorpha); and *Castor*, *Sciurus* and *Guerlinguetus* (Sciuromorpha). Values per taxon are provided in Supplementary Table S3 online.

2.4.2 Load case: Posterior most molar bite

At the molar bite point, Notoungulata generally occupies the medium range of von Mises stress (~0.05–0.12 MPa). Within the order, *Interatherium robustum* and *Pachyrukhos moyani* show the lowest mean stresses (Introb: 0.046; Pacmoy: 0.053 MPa), whereas toxodontids show high values (Adiovi: 0.097 MPa; Nesimb: 0.119 MPa). Similarly high values are recorded in the interatheriids *Miocochilus anomopodus* and *Protypotherium australis*, and the hegetotheriid *Hegetotherium mirabile* (~0.12 MPa). Meanwhile, Mesotheriidae occupy an intermediate position across the order (Pseexi: 0.06–Pleach: 0.09 MPa).

Notoungulata generally exhibits lower stress than most ungulates and diprotodontians, whose mean values reach ~3.0 MPa. Exceptions include *Equus ferus*, *Ceratotherium simum* (Equfer: 0.093; Cersim: 0.13 MPa), *Phacochoerus aethiopicus* (Phaaet: 0.12 MPa), and *Lama glama* (Lamgla: 0.13 MPa), which overlap the notoungulate range (Fig 6).

Among non-ungulates, Hystricomorpha (Hysind: 0.016–Fukliv: 0.037 MPa) and Myomorpha (Musmus: 0.01–Oxycap: 0.18 MPa) generally exhibit lower median stress values than Notoungulata, although their peak stresses are substantially higher. Species such as *Heterohyrax brucei* (0.08 MPa) and *Akodon lindbergh*i (Akolin: 0.093 MPa) displayed stresses like those of mesotheriids, whereas sciuromorphs (Gueing: 0.021–Scivul: 0.084 MPa) showed interquartile and peak values highly comparable to those of notoungulates. Among marsupials, only Wombatidae closely resemble certain notoungulates (Lasssp: 0.05–Vomurs: 0.082 MPa. Values per taxon are provided in Supplementary Table S3 online.

3 Discussion

Palaeoecological categories such as browsing, grazing, digging, and preferences for open versus closed habitats have long underpinned interpretations of notoungulate ecology [13, 14, 16, 17, 19, 21, 25]. These classifications require higher-level inferences about biological roles from morphology [36], but become challenging when all close relatives are extinct, limiting direct functional comparisons within the clade [1]. Our analyses reveal a cohesive notoungulate morphofunctional space distinct from that of extant herbivores. Given the deep phylogenetic isolation of Notoungulata, this pattern highlights the limitations of reconstructing their ecology from modern analogues alone.

Extant herbivores achieve grinding through distinct kinematic patterns, including transverse movements in ungulates and propalinal movements in rodents [30, 37]. Most notoungulates combine mediolaterally expanded articular surfaces and rounded condyles with relatively vertical jaw muscles (Figs. 2–4), consistent with a substantial transverse component combined with predominantly orthal movements, condylar rotation, and a relatively large gape [17, 27, 30, 38]. This partially agrees with previous interpretations of an ungulate-like chewing pattern [22], but differs from living ungulates, in which extensive transverse movements are facilitated by pronounced anisognathy [37]. Most notoungulates instead had upper and lower tooth rows of similar width (see figs. 3–4 [21]; figs. 2–10 [39]; fig. 3 [18].

Although the enlarged masseteric insertion supports a substantial transverse component during mastication [17, 27], the predominantly anterodorsal origin of the masseter in notoungulates [18, 20] generates a greater anteroposterior muscle vector than in most ungulates (Figs. 3a–b and 4b). While this masseter configuration has been described as rodent-like in typotheres [18, 29], their overall masticatory mechanics differ fundamentally from rodents. Notoungulates show relatively lower masseter but higher temporalis MA, reflecting the more vertical orientation of both muscles, whereas rodents combine elongated anteroposterior TMJs with more horizontally oriented muscles (Figs. 2 and 4b–c) that maximize propalinal motion [40]. This combination of orthal and transverse movements provides a functional explanation for the predominantly sub-horizontal microwear striations reported in toxodontids and typotheres [14], while indicating that their masticatory systems were neither equivalent to those of modern ungulates nor truly rodent-like.

This distinctive kinematic configuration was accompanied by high mechanical incisor performance across Notoungulata, supporting previous inferences of powerful anterior biting [21, 41]. Their short, robust anterior mandibular corpus likely enhanced bite-force transmission and structural resistance, while the fused mandibular symphysis would have redistributed loads across both hemimandibles [9, 42]. In contrast, diprotodontians and most artiodactyls exhibit higher stress values, consistent with their elongated rostra, long diastemata, and gracile mandibles (Figs. 1 and 5). Whereas the anterior displacement of the masseter, elevated condyle, and posteriorly inclined ramus increase the moment arm and incisor MA in rodents and wombats (Figs. 1 and 3), only some rodents, with high and posteriorly positioned incisors, overlap the lower end of the Notoungulata stress distribution (Fig. 6) Additionally, typotheres lack the continuous self-sharpening, chisel-like incisors of many rodents [43]. Their semicircular occlusal surfaces [21, 44] support a powerful grasp-and-cut mechanism driven by a strong vertical power stroke rather than prolonged gnawing.

Posterior molar performance shows broadly similar masseter and temporalis MA in Notoungulata and Ungulata, but through different morphologies (Fig. 4). In ungulates, these mechanical advantages are associated with a ventrally positioned condyle and constrained gonial angle, respectively, whereas notoungulates achieve comparable values through a more vertical temporalis and anteriorly positioned masseter (Figs 3a and 4b). Nevertheless, FEA

indicates substantially lower stress in Notoungulata, reflecting greater structural resistance during molar biting due to their stout mandibular body (Fig. 1 and 5). Among extant taxa, *Equus*, *Ceratotherium*, and *Phacochoerus* occupy the closest morphospace to notoungulates, consistent with their low mandibular stress (Fig. 6). Rodents and wombats represent the opposite extreme. In these taxa, anterior masseter displacement shifts the mandibular lever towards a second-class configuration. Combined with a short tooth row, robust corpus, and elevated posterior condyle, this favours high bite force while reducing mandibular stress.

Within Notoungulata, toxodontids show relatively restricted mandibular mobility, consistent with greater condyle–glenoid coupling (see Supplementary Fig. S5 online), although condylar translation beyond the glenoid cavity, as reported in extant ungulates [37], cannot be excluded. Functionally, their TMJ most closely resembles that of tapirs and suids (Fig. 2), which combine condylar rotation with limited anteroposterior and lateromedial translation during mastication [45, 46]. The similarity is particularly strong with tapirs (see Supplementary Fig. S9 online), consistent with proposed phylogenetic affinities between Perissodactyla and Notoungulata [47, 48] and the phylogenetic signal reported for mammalian TMJ morphology [49].

Toxodontids *Nesodon* and *Adinotherium*, interpreted as browsers based on microwear, likely incorporated mechanically resistant foods [22]. If grazing requires greater masticatory efficiency than browsing [12], our results broadly support this distinction, with toxodontids showing lower mechanical performance associated with their elongated mandibular corpus and more acute mandibular angle (Fig. 1; see Supplementary Fig. S2 online). This pattern may also reflect adaptive scaling, whereby smaller-bodied typotheres compensate for lower absolute force generation through more robust and efficient mandibular architectures.

Mesotheriids illustrate a related pattern. Their short mandibular bodies and relatively obtuse corpus–ramus angles increase masseter MA and contribute to the highest incisor performance within Notoungulata (Figs. 3 and 5), consistent with previous interpretations of hard-item processing in Miocene representatives. Nevertheless, mesotheriids occupy a relatively conservative region of morphospace and show broadly similar mechanical properties across taxa, including the derived bulk–grazer *Mesotherium cristatum* [21]. The broader rostrum of later representatives [44, 50] may therefore reflect dietary broadening without a major reorganization of the underlying masticatory system.

Other typotheres show greater functional differentiation. The lower anterior bite performance of *Hegetotherium mirabile* may reflect its horizontally elongated incisors and hypertrophied upper incisors, forming a chisel-like apparatus proposed for exploiting decaying wood [26]. Despite retaining a generalized notoungulate TMJ, its enlarged anterior masseter and reduced temporalis suggest controlled transverse movements (Fig. 2–4). Although compatible with a grazing interpretation [17], its distinctive cranio-dental morphology (Fig. 1) suggests broader ecological specialization. The proposed wood-feeding behaviour remains plausible but requires direct dietary evidence.

Pachyrukhos represents an even more distinctive condition, combining rounded articular surfaces with an anteriorly positioned masseter and increased mandibular mobility (Fig. 2). Its estimated anteroposterior mobility, however, remains below that of most sciuromorph rodents (see Supplementary Figs. S6–S8 online), indicating that its masticatory system was specialized relative to other notoungulates but did not reproduce the full propalinal condition of rodents. Recent dietary evidence for greater seed and fruit consumption and a reduced contribution of grasses is therefore consistent with increased functional versatility rather than direct rodent-like convergence [18, 25].

Interatheriidae shows the greatest biomechanical disparity within Notoungulata. *Interatherium robustum* exhibits the lowest overall mechanical stress, comparable only to the hegetotheriid *Pachyrukhos* during molar biting. Thus, interpreting *I. robustum* and *P. australis* as primarily grazers [17] may oversimplify functional variation within Interatheriidae. The short, deep corpus and elevated tooth row of *I. robustum* instead approach a sciuromorph-like configuration associated with processing mechanically resistant resources (Figs. 1, 5 and 6; [43], including hard seeds and tough vegetation.

By contrast, *Protypotherium* australis and *Miocochilius anomopodus* show lower mechanical efficiency (Fig. 6), consistent with less mechanically demanding plant resources, as suggested by microwear in *Protypotherium* [22]. In *P. australis*, the anteriorly positioned condyle favors incisor force transmission but, together with its gracile posterior corpus, reduces resistance during molar biting. *M. anomopodus* shows the poorest performance, with the highest stress at both bite regions, consistent with its elongated corpus and ventrally positioned condyle, which approach a generalized ungulate configuration (Figs. 1, 5, and 6).

Interestingly, *Heterohyrax* and *Ceratotherium* are the closest extant functional analogues based on mandibular shape (Fig. 1), showing similar stress distributions (Figs. 5 and 6), consistent with previous suggestions of functional similarity [9, 13]. Like notoungulates, both retain a relatively extensive temporalis insertion compared with most ungulates [27] yet represent contrasting dietary strategies: *Heterohyrax* is a specialized browser, whereas *Ceratotherium* is an obligate grazer [51, 52]. This contrast highlights the limited capacity of mandibular shape alone to predict diet. The functional resemblance of the notoungulate TMJ to those of suids and tapirs further supports a generalized feeding strategy, consistent with the capacity to process diverse plant resources, including leaves, shoots, fruits, seeds, grasses, and bark [46, 53].

Together, these patterns show that evolutionary convergence provides a useful framework for reconstructing the paleodiets of extinct mammals, but that no single extant analogue adequately captures the notoungulate feeding system. Instead, different components of the feeding apparatus converge on different herbivorous lineages: incisor performance overlaps with sciuromorph rodents, molar mechanics approach those of ungulates, mandibular shape resembles hyracoids and rhinoceroses, and TMJ architecture converges with generalized herbivores such as suids and tapirs. Recurrent affinities with perissodactyls may additionally reflect deeper evolutionary history within Panperissodactyla [47, 48]. Rather than indicating ecological equivalence, these partial affinities reveal a mosaic evolutionary solution in which functionally disparate traits were integrated into a distinctive masticatory system, reflecting a lineage-specific evolutionary pathway within one of South America's most distinctive endemic mammalian radiations.

4 Materials and Methods

4.1 Data base

The sample comprised 128 lateral view 2D images of the craniomandibular region from extant primarily herbivorous placental and marsupial mammals: ungulates from the families Bovidae (n=34), Cervidae (6), Suidae (5), Camelidae (1), Tragulidae (1), Giraffidae (1), Rhinocerotidae (1), Equidae (1), and Tapiridae (3). Rodents organised as Hystricomorpha (25), Myomorpha (28), and Sciuromorpha (11) [54]. Leporidae (2), Hyracoidea (1); and the marsupials: Wombatidae (2), Macropodidae (3), Pseudocheiridae (1), Potoroidae (1), and Phalangeridae (1), all belonging to Diprotodontia. However, the name 'Diprotodontia' is used exclusively for

non-wombat diprotodontians. Each specimen represented a different taxon; therefore, intraspecific variation was not considered.

We included images of 12 notoungulate taxa, obtained both from published sources and distinct research collections: Toxodontia (3, late Oligocene to middle Miocene) and from Typotheria: Mesotheriidae (4, late Miocene–early Pleistocene), Interatheriidae (3, early to middle Miocene), Hegetotheriidae (2, early to middle Miocene). For figures, taxa were coded using six-letter abbreviations comprising the first three letters of the genus and specific epithet (see Supplementary Table S1 online).

4.2 Geometric morphometrics

Mandibular shape was analysed using two-dimensional geometric morphometrics. Landmarks (lm) and semi landmarks (slm) were taken using TPSdig2 v.2.31 [55] and selected to capture anatomical homology and biomechanical features, including incisors orientation (lm 12-14), diastema extent (lm 11-12), corpus height (lm/slm 9-11; 15-17), gonial angle acuteness (lm/slm 18-24), condyle relative placement (lm/slm 1-3), coronoid height and/or orientation (lm/slm 3-9) (see Supplementary Fig. 10 and Table S2 online). We included teeth as a part of the mandible unit, because it enhances dimensional features in 2D, such as maximum height, length, given curvatures and relative angles on the cartesian plane, which are contributing to the general masticatory performance. Raw coordinates were imported into MorphoJ v1.06d software, and Procrustes superimposition was applied [56]. Then, a principal component analysis (PCA) was carried out in MorphoJ, to explore the distribution of the shape diversity.

The effect of allometry was assessed by calculating R^2 from a linear regression of log centroid size against Procrustes coordinates, using 10,000 permutations to test significance. Regression residuals were then extracted to represent shape variation independent of allometric effects [57], and a new covariance matrix and size-corrected PCA were generated.

4.3 Temporo-mandibular joint functional index

We assessed mandibular rotation and anteroposterior/lateromedial translation using linear measurements obtained in ImageJ [58]. First, joint rotation was assessed on the condyle in lateral view using the condylar curvature index (CCI), calculated as the proportion between a chord drawn along the condyle perimeter and the distance between the extremes of this chord. Greater condylar convexity was interpreted as facilitating rotation, whereas flatter condyles were assumed to constrain it [35, 59].

Second, we evaluated the correlation between the condylar index (CI) and glenoid cavity index (GCI) using Spearman rank correlation (see Supplementary Fig. S5 online). CI was calculated as the ratio of the longitudinal to transverse axes of the condyle in dorsal view, whereas GCI was calculated using the same proportions for the glenoid cavity in ventral view (see Supplementary Fig. S10 online). The predominant joint axis should reflect the main direction of mandibular movement during occlusion, whereas a weak correlation between CI and GCI would indicate greater potential for complex translational movements of the TMJ [26, 59, 35].

To assess morphological disparity and potential convergence in TMJ functional indices, we performed a non-hierarchical k-means cluster analysis [60] based on pairwise Euclidean distances in R version 4.5.1 [61]. The optimal number of clusters was determined using the "alllong" index in the NbClust package [62], which indicated two or three clusters; we selected three to improve visualization. Given the non-parametric nature of our data (Shapiro–Wilk, p

< 0.05), differences among clusters were tested using PERMANOVA with 10,000 permutations. All calculated index values are provided in Supplementary Table S3 online.

4.4 Mechanical advantage

Masseter and temporalis muscle force vectors were reconstructed by aligning 2D mandible and skull images in dental occlusion using GIMP v3.0.6 and importing them into Rhinoceros v4.0 [63]. Muscle outlines were traced based on muscle scar topography, published dissections and segmented 3D CT images, comparative data from herbivorous mammals, and previous reconstructions of masticatory muscles in notoungulates (see references in SI Appendix). Muscle centroids were calculated using the *AreaCentroid* command in Rhinoceros v4.0, and force vectors were defined from the midpoint of the mandibular attachment area to each centroid. All vectors were digitized twice by a single operator (JIAD) to assess repeatability and minimize spurious vectors.

Mechanical advantage (MA= Mi/Mo) was calculated as the ratio of the input moment arm (Mi), which is the perpendicular distance of the muscle force vector to the pivot (TMJ) and the output moment arm (Mo). The latter was defined based on four different bite points: the incisor bite (BP1); the anterior tip of the first tooth after the diastema (BP2); the mid distance between BP2 and BP4 (BP3); the posterior tip of the last molar (BP4). Results were expressed as a percentage (See Supplementary Fig. S10 and Supplementary Table S3 for the calculated values for each bite).

4.5 Finite Element Analyses

Bidimensional models were generated in Rhinoceros v4.0 by tracing closed polylines around mandibular and dental outlines and initially meshing them using the *meshpolyline* command, followed by refinement in 3-Matic Research 10.0 x64 [64] to obtain regular triangular elements with 0.5–1.0 mm side lengths. To determine the appropriate mesh size between 2,000 and 10,000 elements, a Kruskal–Wallis test with Bonferroni adjustment was performed. Results indicated that ~5,000 elements provided reliable results while optimizing calculation speed and retaining sufficient anatomical detail (see Supplementary Fig. S11 online).

Models were imported into Strand7 [65] and configured as shell surfaces composed of plate elements, aligned horizontally and projected onto a cylindrical coordinate system (r, θ, z), with the origin at the condyle, which was constrained along alla axes except θ, allowing dorsoventral mandibular rotation corresponding to mouth opening and closing. Models were scaled to a standardized longitudinal length of 20 cm and assigned a thickness of 2 cm.

Masseter and temporalis insertion areas were defined by networks of interconnected links evenly distributed across the corresponding surfaces and represented by beam elements created by extruding the node closest to the origin of each muscle vector, using the same orientation and length as in the previous MA analyses. The distal node of each beam was constrained in all degrees of freedom.

Four loading cases were generated by applying a −100 N force in the axial (z) direction at each bite point (BP1–BP4). Material properties were assigned as follows: shell plates were modelled as isotropic Haversian bone (ρ = 1,895 kg/m³, E = 10 GPa, ν = 0.3; [66]), while muscle beam elements received standard soft-tissue values (ρ = 1,200 kg/m³, E = 350 kPa, ν = 0.47; [67]). All calculations used von Mises stress, widely applied to assess the mechanical behaviour of bone under load [68].

Stress results were analysed in two regions: the anterior mandibular body, from the incisor to the posterior end of the diastema (incisor bite), and the posterior mandibular body, from the posterior end of the diastema to the posterior edge of the tooth row (molar bite; see Supplementary Fig. S10 and Table S3 online). To avoid numerical singularities, 5% of peak stress values were excluded [69].

5 References

1. Lauder, G.V. On the inference of function from structure in *Functional Morphology in Vertebrate Paleontology* (ed. Thomason J.J.) 1–18 (Cambridge University Press 1995).
2. Simpson, G. G. The beginning of the age of mammals in South America. Part I. *Bull. Am. Mus. Nat. Hist.* **91,** 1–232 (1948).
3. Bond, M. E., Cerdeño, E. & López, G. Los ungulados nativos de América del Sur in *Evolución biológica y climática de la región pampeana durante los últimos cinco millones de años* (eds. Alberdi, M. T., Leone, G. & Tonni, E. P.) 259–292 (Museo Nacional de Ciencias Naturales, Consejo Superior de Investigaciones Científicas, 1995).
4. Solórzano, A., Núñez-Flores, M. & Rodríguez-Serrano, E. The rise and fall of notoungulates: How Andean uplift, available land area, competition, and depredation driven its diversification dynamics. *Gondwana Res.* **135,** 116-132; https://doi.org/10.1016/j.gr.2024.08.002 (2024).
5. Simpson, G. G. *Splendid Isolation: The Curious History of South American Mammals* (Yale University Press, 1980).
6. McKenna, M. C. & Bell, S. K. *Classification of Mammals Above the Species Level* (Columbia University Press, 1997).
7. Croft, D. A., Gelfo, J. N. & López, G. M. Splendid innovation: the extinct South American native ungulates. *Annu. Rev. Earth Planet. Sci.* **48,** 259-290; https://doi.org/10.1146/annurev-earth-072619-060126 (2020).
8. Zittel, K. A. *Grundzüge der Paläontologie* (Paläozoologie) 518–527 (R. Oldenbourg, 1895).
9. Sinclair, W. J. Typotheria of the Santa Cruz Beds in *Reports of the Princeton University Expeditions to Patagonia*, 1896–1899, vol. VI (ed. Scott, W.B.) 1–109 (Princeton University, 1909)
10. Patterson, B., On the auditory region of the Toxodontia. Field Mus Nat Hist, Geol Ser 6, 1–27 (1932).
11. Cifelli, R. L., The phylogeny of the native South American ungulates in *Mammal Phylogeny*, *Volume 2: Placentals* (eds. Szalay, F. S., Novacek, M. J. & McKenna, M. C.) 195–216 (Springer-Verlag, 1993).
12. Janis, C. M. An evolutionary history of browsing and grazing ungulates in *The Ecology of Browsing and Grazing* (eds. Gordon, I. J. & Prins, H. H. T.) 21–42 (Springer, 2008).
13. Shockey, B. J., Croft, D. A. & Anaya, F. Analysis of function in the absence of extant functional homologues: A case study using mesotheriid notoungulates (Mammalia). *Paleobiology* **33,** 227–247; https://doi.org/10.1666/05052.1 (2007).
14. Billet, G., Blondel, C. & de Muizon, C. Dental microwear analysis of notoungulates (Mammalia) from Salla (Late Oligocene, Bolivia) and discussion on their precocious hypsodonty. *Palaeogeogr. Palaeoclimatol. Palaeoecol.* **274,** 114–124; https://doi.org/10.1016/j.palaeo.2009.01.004 (2009).
15. Reguero, M. A., Candela, A. M. & Cassini, G. H. Hypsodonty and body size in rodent-like notoungulates in *The Paleontology of Gran Barranca: Evolution and Environmental Change through the Middle Cenozoic of Patagonia* (eds. Madden, R.

H., Carlini, A. A., Vucetich, M. G. & Kay, R. F.) 358–367 (Cambridge University Press, 2010).
16. Gomes-Rodrigues, H., Herrel, A. & Billet, G. Ontogenetic and life history trait changes associated with convergent ecological specializations in extinct ungulate mammals. *Proc. Natl. Acad. Sci.* U.S.A. **114,** 1069–1074; https://doi.org/10.1073/pnas.1614029114 (2017).
17. Cassini, G. H. & Vizcaíno, S. F. An approach to the biomechanics of the masticatory apparatus of Early Miocene (Santacrucian Age) South American ungulates (Astrapotheria, Litopterna, and Notoungulata): Moment arm estimation based on 3D landmarks. *J. Mamm. Evol.* **19,** 9–25; https://doi.org/10.1007/s10914-011-9179-5 (2012).
18. Ercoli, M. D., Álvarez, A. & Candela, A. M. Sciuromorphy outside rodents reveals an ecomorphological convergence between squirrels and extinct South American ungulates. *Commun. Biol.* **2,** 202; https://doi.org/10.1038/s42003-019-0423-5 (2019).
19. Cassini, G. H., Mendoza, M., Vizcaíno, S. F. & Bargo, M. S. Inferring habitat and feeding behaviour of early Miocene notoungulates from Patagonia. *Lethaia* **44,** 153–165; https://doi.org/10.1111/j.1502-3931.2010.00231.x (2011).
20. Cassini, G. H. Paleobiología de ungulados de la Formación Santa Cruz (Mioceno temprano-medio), Patagonia, Argentina: una aproximación morfométrica y morfofuncional al estudio del aparato masticatorio. PhD thesis, Universidad Nacional de la Plata, Argentina at https://sedici.unlp.edu.ar/handle/10915/82878 (2011).
21. Ercoli, M. D. & Armella, M. A. Snout shape and masticatory apparatus of the rodent-like mesotheriid ungulates (Notoungulata, Typotheria): Exploring evolutionary trends in dietary strategies through ancestral reconstructions. *Palaeontology* **64,** 385–408; https://doi.org/10.1111/pala.12530 (2021).
22. Townsend, K. B. & Croft, D. A. Diets of notoungulates from the Santa Cruz Formation, Argentina: New evidence from enamel microwear. *J. Vertebr. Paleontol.* **28,** 217–230; https://doi.org/10.1671/0272-4634(2008)28[217:DONFTS]2.0.CO;2 (2008).
23. Cassini, G. H., Vizcaíno, S. F. & Bargo, M. S. Body mass estimation in Early Miocene native South American ungulates: A predictive equation based on 3D landmarks. *J. Zool.* **287,** 53–64; https://doi.org/10.1111/j.1469-7998.2011.00886.x (2012).
24. Ercoli, M. D., Álvarez, A., Moyano, S. R., Youlatos, D. & Candela, A. M. Tracing the paleobiology of Paedotherium and Tremacyllus (Pachyrukhinae, Notoungulata), the latest sciuromorph South American native ungulates—Part I: Snout and masticatory apparatus. *J. Mamm. Evol.* **28,** 377–409; https://doi.org/10.1007/s10914-020-09518-5 (2021).
25. Armella, M.A. & Croft, D. A. Pass on the grass? The unexpected "last supper" of hypselodont Pachyrukhinae (Notoungulata, Mammalia) from the late Neogene of northwestern Argentina. *Palaeogeogr. Palaeoclimatol. Palaeoecol.* **687,** 113585; https://doi.org/10.1016/j.palaeo.2026.113585 (2026).
26. McCoy, D. E. & Norris, C. A. The cranial anatomy of the Miocene notoungulate Hegetotherium mirabile (Notoungulata, Hegetotheriidae) with preliminary observations on diet and method of feeding. *Bull. Peabody Mus. Nat. Hist.* **53,** 355–374 (2012).
27. Turnbull, W. D. Mammalian masticatory apparatus. *Fieldiana Geol.* **18,** 149–356; https://doi.org/10.5962/bhl.title.5442 (1970).
28. Croft, D. A. & Weinstein, D. The first application of the mesowear method to endemic South American ungulates (Notoungulata). *Palaeogeogr. Palaeoclimatol. Palaeoecol.* **269,** 103–114; https://doi.org/10.1016/j.palaeo.2008.08.007 (2008).

29. Sosa, L. M. & García-López, D. A. Structural variation of the masseter muscle in Typotheria (Mammalia, Notoungulata). *Ser. Correl. Geol.* **34,** 53–70; https://doi.org/10.5281/zenodo.5095268 (2018).
30. Popowics, T. E. & Herring, S. W. Teeth, jaws and muscles in mammalian mastication in *Feeding in Domestic Vertebrates: From Structure to Behaviour* (ed. Bels, V.) 61–83 (CABI, 2006).
31. Cassini, G. H. Skull geometric morphometrics and paleoecology of Santacrucian (late early Miocene; Patagonia) native ungulates (Astrapotheria, Litopterna, and Notoungulata). *Ameghiniana* **50,** 193–216; https://doi.org/10.5710/AMGH.7.04.2013.606 (2013).
32. Scott, W. B., Mammalia of the Santa Cruz beds. Part 2: Toxodonta in *Reports of the Princeton University Expeditions to Patagonia, 1896–1899*, (ed. Scott, W. B.)111–238 (Princeton University, 1912).
33. MacFadden, B. J. & Shockey, B. J. Ancient feeding ecology and niche differentiation of Pleistocene mammalian herbivores from Tarija, Bolivia: Morphological and isotopic evidence. *Paleobiology* **23,** 77–100; https://doi.org/10.1017/S009483730001665 (1997).
34. Medina-González, P. & Moreno, K. Morphofunctional space of the forelimb in *Caraguatypotherium munozi* (Notoungulata; Mesotheriidae): insights into wrist-powered digging. *J. Morphol.* **286,** e70069; https://doi.org/10.1002/jmor.70069 (2025).
35. Terhune, C. E. Dietary correlates of temporomandibular joint morphology in New World primates. *J. Hum. Evol.* **61,** 583–596; https://doi.org/10.1016/j.jhevol.2011.08.003 (2011).
36. Vizcaíno, S. F., Bargo, M. S., Cassini, G. H. & Toledo, N. Forma y función en paleobiología de vertebrados (Editorial de la Universidad Nacional de La Plata, 2016).
37. Weijs, W. A. Evolutionary approach of masticatory motor patterns in mammals in *Biomechanics of Feeding in Vertebrates* (eds. Bels, V. L., Chardon, M. & Vandewalle, P.) 281–314 (Springer, 1994).
38. Maynard Smith, J. & Savage, R. J. G. The mechanics of mammalian jaws. *Sch. Sci. Rev.* **40,** 289–301 (1959).
39. Fernández, M. & Muñoz, N. A. Notoungulata and astrapotheria (Mammalia, meridiungulata) of the Santa Cruz Formation (early middle Miocene) along the Río Santa Cruz, Argentine Patagonia. *PEAPA* **19,** 138–169; https://doi.org/10.5710/PEAPA.19.09.2019.288 (2019).
40. Satoh, K. Comparative functional morphology of mandibular forward movement during mastication of two murid rodents, Apodemus speciosus (Murinae) and Clethrionomys rufocanus (Arvicolinae). *J. Morphol.* **231,** 131–142; https://doi.org/10.1002/(SICI)1097-4687(199702)231:23.0.CO;2-H (1997).
41. Filippo, A., Kalthoff, D. C., Billet, G. & Gomes-Rodrigues, H. Evolutionary and functional implications of incisor enamel microstructure diversity in Notoungulata (Placentalia, Mammalia). *J. Mamm. Evol.* **27,** 211–236; https://doi.org/10.1007/s10914-019-09462-z (2020).
42. Ravosa, M. J. & Vinyard, C. J. Masticatory loading and ossification of the mandibular symphysis during anthropoid origins. *Sci. Rep.* **10,** 5950; https://doi.org/10.1038/s41598-020-62025-8 (2020).
43. Samuels, J. X. Cranial morphology and dietary habits of rodents. *Zool. J. Linn. Soc.* **156,** 864–888; https://doi.org/10.1111/j.1096-3642.2009.00502.x (2009).
44. Fernández-Monescillo, M., Croft, D. A., Pujos, F. & Antoine, P.-O. Taxonomic history and intraspecific analysis of Mesotherium cristatum (Mammalia, Notoungulata,

Mesotheriidae) from the Early-Middle Pleistocene of Buenos Aires Province, Argentina. *Hist. Biol.* **35,** 1028–1040; https://doi.org/10.1080/08912963.2022.2074844 (2023).
45. Menegaz, R. A., Baier, D. B., Metzger, K. A., Herring, S. W. & Brainerd, E. L. XROMM analysis of tooth occlusion and temporomandibular joint kinematics during feeding in juvenile miniature pigs. *J. Exp. Biol.* **218,** 2573–2584; https://doi.org/10.1242/jeb.119438 (2015).
46. Hohl, C. J. et al. Chewing, dental morphology and wear in tapirs (Tapirus spp.) and a comparison of free-ranging and captive specimens. *PLoS One* **15,** e0234826; https://doi.org/10.1371/journal.pone.0234826 (2020).
47. Buckley, M. Ancient collagen reveals evolutionary history of the endemic South American 'ungulates'. *Proc. R. Soc. B* **282,** 20142671; https://doi.org/10.1098/rspb.2014.2671 (2015).
48. Welker, F. et al. Ancient proteins resolve the evolutionary history of Darwin's South American ungulates. *Nature* **522,** 81–84; https://doi.org/10.1038/nature14249 (2015).
49. Terhune, C. E., Mitchell, D. R., Cooke, S. B., Kirchhoff, C. A. & Massey, J. S. Temporomandibular joint shape in anthropoid primates varies widely and is patterned by size and phylogeny. *Anat. Rec.* **305,** 2227–2248; https://doi.org/10.1002/ar.24886 (2022).
50. Fernández-Monescillo, M. & Tauber, A. A. Beyond extinction: Uncovering morphological aspects of the last typotherid population (Mesotherium cristatum) and the unexpected body mass decrease. *Quat. Sci. Rev.* **325,** 108479; https://doi.org/10.1016/j.quascirev.2023.108479 (2024).
51. Barry, R. E. & Shoshani, J. Heterohyrax brucei. *Mamm. Species* **645,** 1–7; https://doi.org/10.1644/0.645.1 (2000).
52. Steuer, P. et al. Comparative investigations on digestion in grazing (*Ceratotherium simum*) and browsing (*Diceros bicornis*) rhinoceroses. *Comp. Biochem. Physiol. A Mol. Integr. Physiol.* **156,** 380–388; https://doi.org/10.1016/j.cbpa.2010.03.006 (2010).
53. Herring, S. W. TMJ anatomy and animal models. *J. Musculoskelet. Neuronal Interact.* **3,** 391–394 (2003).
54. Cox, P. G. & Jeffery, N. Reviewing the morphology of the jaw-closing musculature in squirrels, rats, and guinea pigs with contrast-enhanced microCT. *Anat. Rec.* **294,** 915–928; https://doi.org/10.1002/ar.21381 (2011).
55. Rohlf, F. J. TPSdig, version 2.17 (Stony Brook University, 2013).
56. Klingenberg, C. P. MorphoJ: An integrated software package for geometric morphometrics. *Mol. Ecol. Resour.* **11,** 353–357; https://doi.org/10.1111/j.1755-0998.2010.02924.x (2011).
57. Klingenberg, C. P. Size, shape, and form: Concepts of allometry in geometric morphometrics. *Dev. Genes Evol.* **226,** 113–137; https://doi.org/10.1007/s00427-016-0539-2 (2016).
58. Schneider, C. A., Rasband, W. S. & Eliceiri, K. W. NIH Image to ImageJ: 25 years of image analysis. *Nat. Methods* **9,** 671–675; https://doi.org/10.1038/nmeth.2089 (2012).
59. Vallittu, P. K. et al. Temporomandibular joint and giant panda's (Ailuropoda melanoleuca) adaptation to bamboo diet. *Sci. Rep.* **11,** 14252; https://doi.org/10.1038/s41598-021-93808-2 (2021).
60. MacQueen, J. Some methods for classification and analysis of multivariate observations in *Proc. 5th Berkeley Symp. Math. Stat. Probab.* (eds. Le Cam, L. M. & Neyman, J.) 281–297 (University of California Press, 1967).
61. R Core Team. R: A language and environment for statistical computing, version 4.5.1 (R Foundation for Statistical Computing, 2025).

62. Charrad, M., Ghazzali, N., Boiteau, V. & Niknafs, A. NbClust: An R package for determining the relevant number of clusters in a data set. *J. Stat. Softw.* **61,** 1–36; https://doi.org/10.18637/jss.v061.i06 (2014).
63. R. McNeel & Associates. Rhinoceros 3D, version 4.0 (Robert McNeel & Associates, 2008).
64. Materialise. 3-matic Research, version 10.0 (Materialise NV, 2015).
65. Strand7 Pty Ltd. Strand7, release 2.4.6, build 4 (Strand7 Pty Ltd., 2018).
66. Reilly, D. T. & Burstein, A. H. The elastic and ultimate properties of compact bone tissue. *J. Biomech.* **8,** 393–405 (1975).
67. Currey, J. D. Bones: Structure and Mechanics (Princeton University Press, 2002).
68. Marcé-Nogué, J. Mandibular biomechanics as a key factor to understand diet in mammals in *Mammalian Teeth: Form and Function* (eds. Martin, T. & von Koenigswald, W.) 55–80 (Verlag Dr. Friedrich Pfeil, 2020)
69. Marcé-Nogué, J., Püschel, T. A. & Kaiser, T. M. A biomechanical approach to understand the ecomorphological relationship between primate mandibles and diet. *Sci. Rep.* **7,** 8364; https://doi.org/10.1038/s41598-017-08161-0 (2017).

6. Acknowledgements

We thank the Santos family (Jimena Ramírez, Fabián Santos, José Carlos Santos and Carlos Santos) for their invaluable help with fieldwork and fossil collection at Caragua. We thank the Mammalogy Collection of the Universidad Austral de Chile for access to comparative material, and Germán Montoya for facilitating additional comparative material. We thank the Department of Veterinary Anatomy at the Universidad Austral de Chile for access to comparative osteological material, and Karina Buldrini and the Museo Nacional de Historia Natural (MNHN), Santiago de Chile, for access to notoungulate fossil collections and photographic data.

7. Author contributions

JIAD: Conceptualization, methodology, investigation, formal analysis, software, visualization, and writing-original draft preparation; KK: Validation, writing—review and editing; MF-M: Validation, writing-review and editing; KM: Conceptualization, methodology, investigation, software, and writing-review and editing.

8. Data Availability statement

The data supporting the findings of this study are provided in the Supplementary Information. Additional data are available from the corresponding author upon reasonable request.

9. Additional Information

Supplementary Information is available in the online version of this paper.

Competing Interests: The authors declare no competing interests.

10. Funding Declaration

The study is supported by the Fondecyt project 1240805 “advancing in our understanding in mesotheriid feeding ecology”, and by the PANPERISSOEVO project, funded through the César Nombela Atracción de Talento programme of the Comunidad de Madrid (2023-T1/ECO-29191) to MF-M

11. Figures

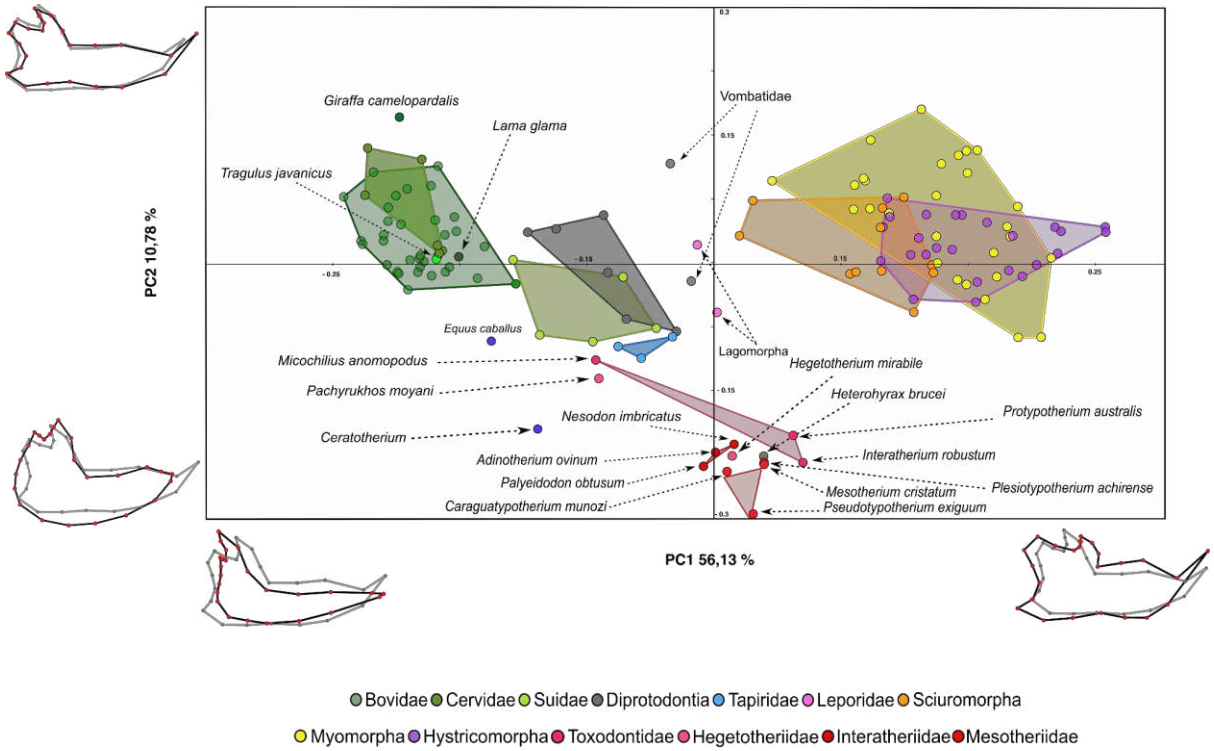


Fig. 1. Principal component analysis of mandibular shape variation in notoungulates and extant herbivores. Morphospace showing warped mandible meshes at PC extremes (PC1 and PC2). Gray wireframes represent the generalized shape.

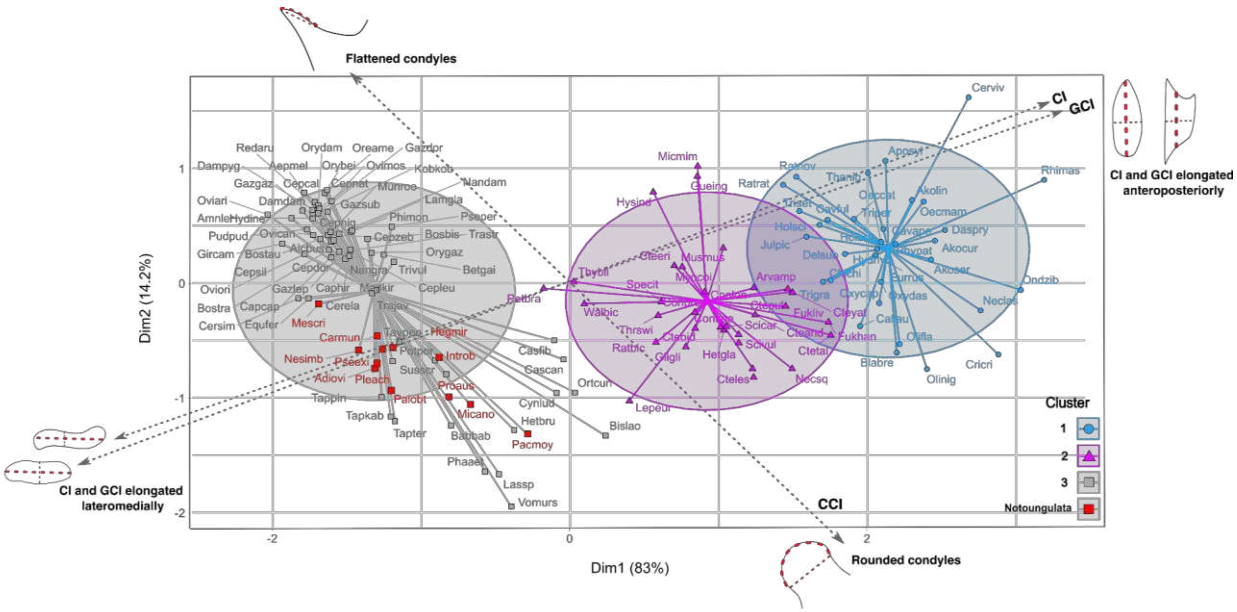


Fig. 2. Non-hierarchical cluster analysis. Cluster 1: species with anteroposterior elongated condyles and glenoid cavities; Cluster 2: species with nearly circular condyles; Cluster 3: species characterized by strongly

lateromedially expanded articular surfaces. Species abbreviations are provided in Table S1 of the electronic supplementary material.

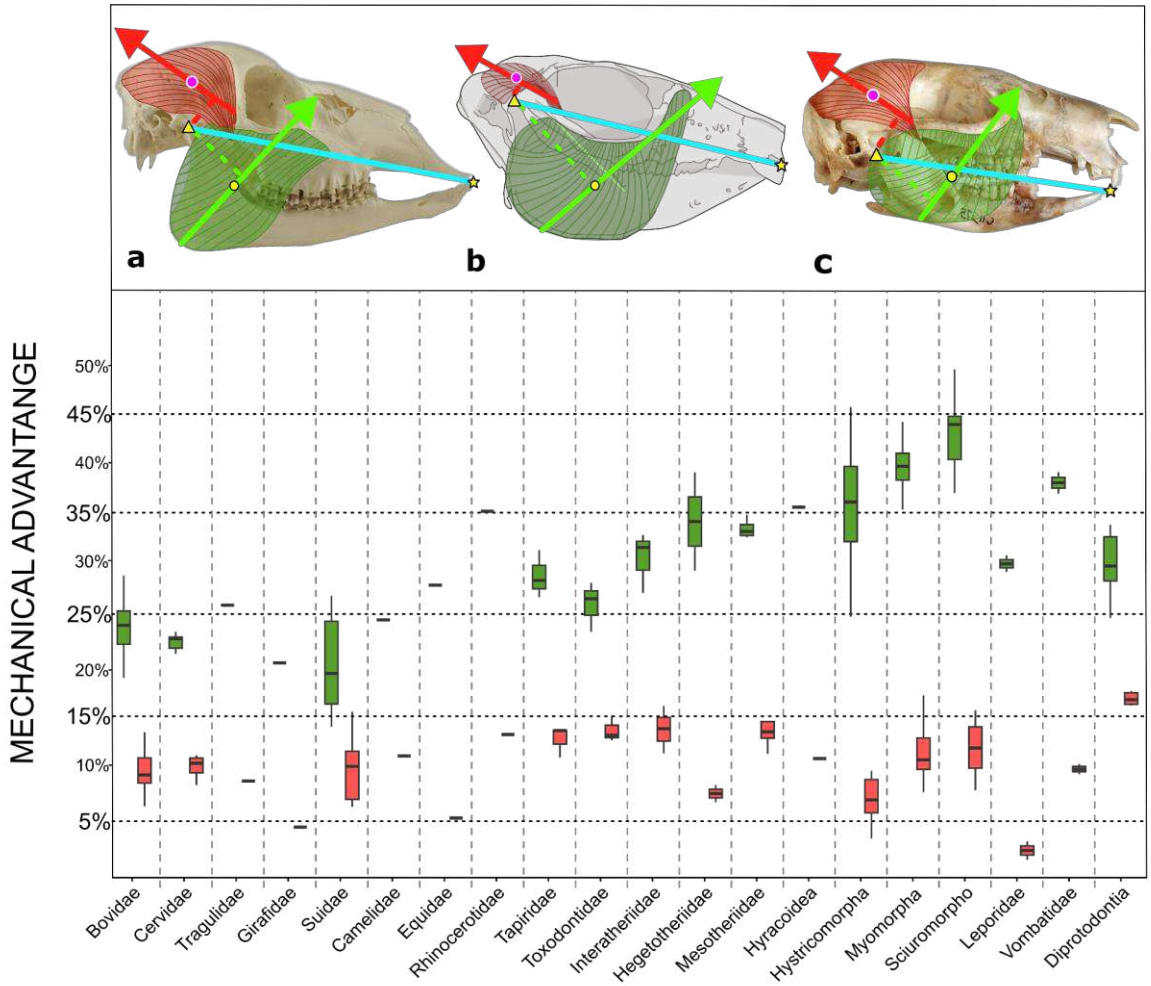
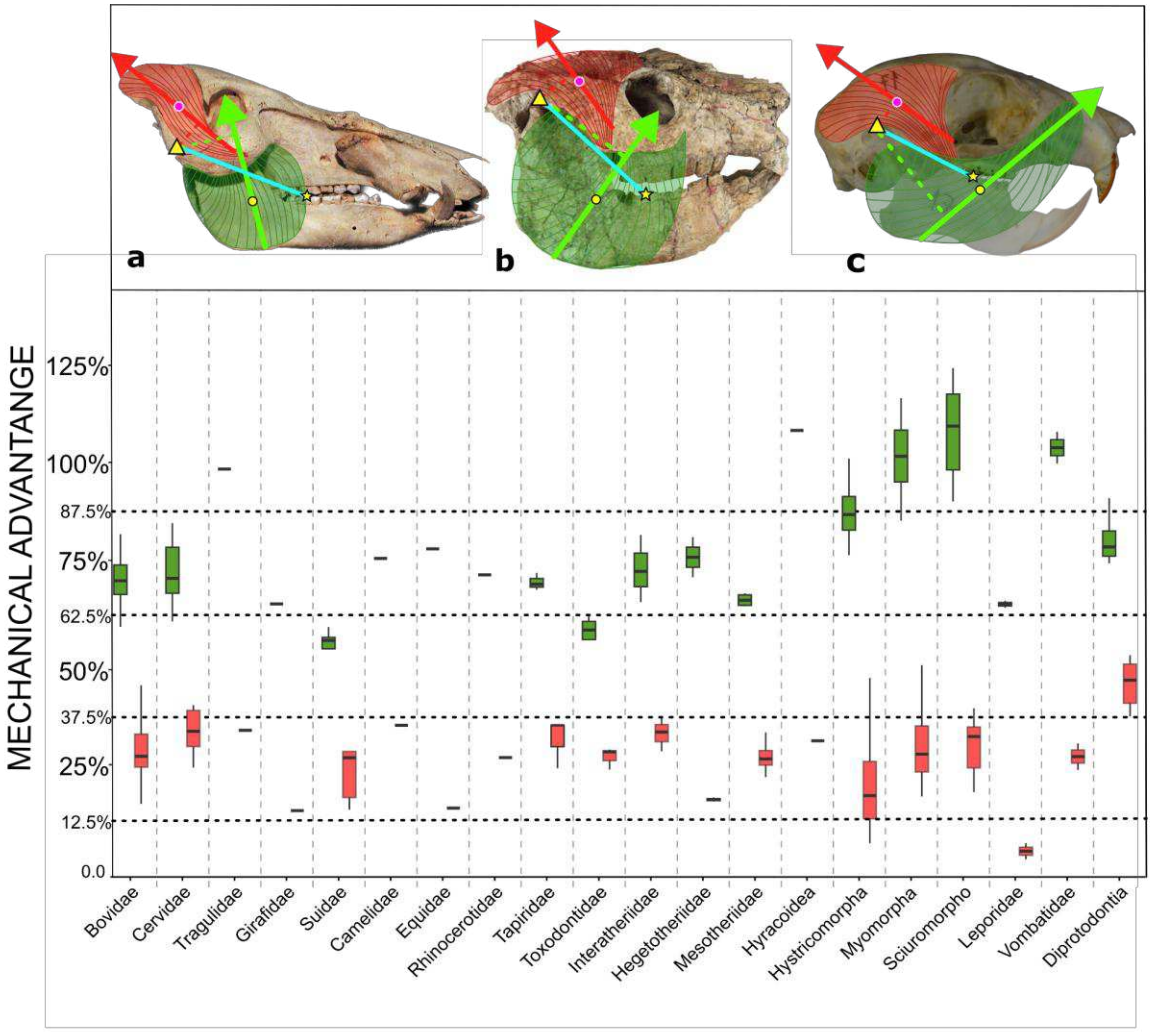


Fig. 3. Mechanical advantage of the masseter (green) and temporalis (red) at the incisor bite point (BP1). a) *Cervus elaphus* (Cervidae, modified from skullbase.info by Ádám Pereszlényi), b) *Pachyrukhos moyani* (Hegetotheriidae; Modified from Sinclair, 1909), c) *Thylogale ballierdi* (Macropodidae modified from Museums Victoria, 118175). Muscle moment arm (dotted line). Resistance moment arm (cyan). Centroid of each masticatory (yellow and pink circles). Dotted lines define the lowest, medium, and upper range in both temporalis and masseter muscles. Temporomandibular joint (fulcrum; yellow triangle).



729
730 **Fig. 4.** Mechanical advantage of the masseter (green) and temporalis (red) at the molar bite point (BP4). a)
731 *Potamochoerus porcus* (Suidae, modified by Rebecca A. Banasiak, FMNH 98099) b) *Caraguatypotherium*
732 *munozi* (Mesotheriidae, Huay-16-100 science earth institute, GEO-UACH) c) *Guerlinguetus ingrami*
733 (Sciuromorpha by Thamila Barcellos, UFES 17). Muscle moment arm (dotted line). Resistance moment arm
734 (cyan). Centroid of each masticatory (yellow and pink circles). Dotted lines define the lowest, medium, and upper
735 range in both temporalis and masseter muscles. Temporomandibular joint (fulcrum; yellow triangle).

736

737

738

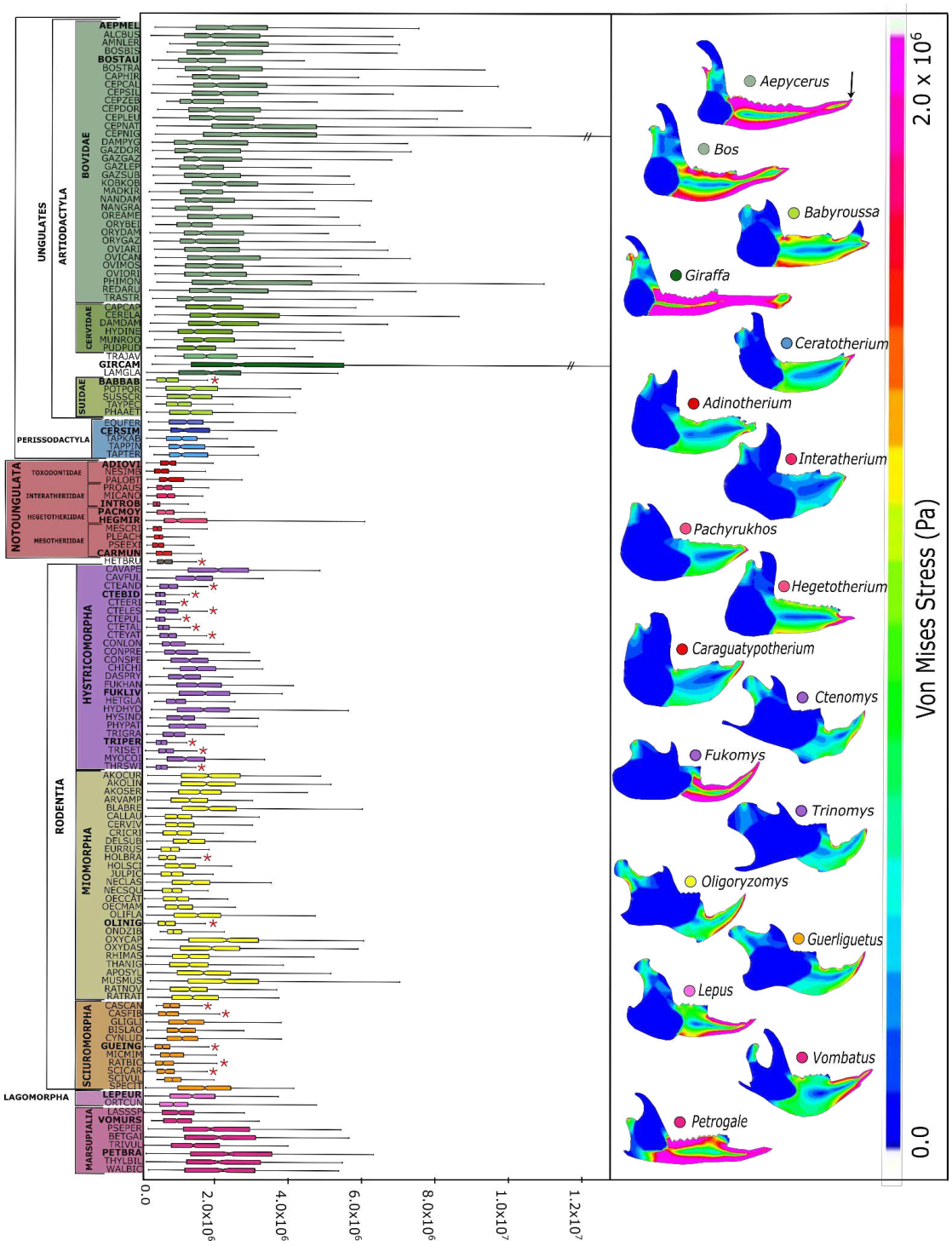
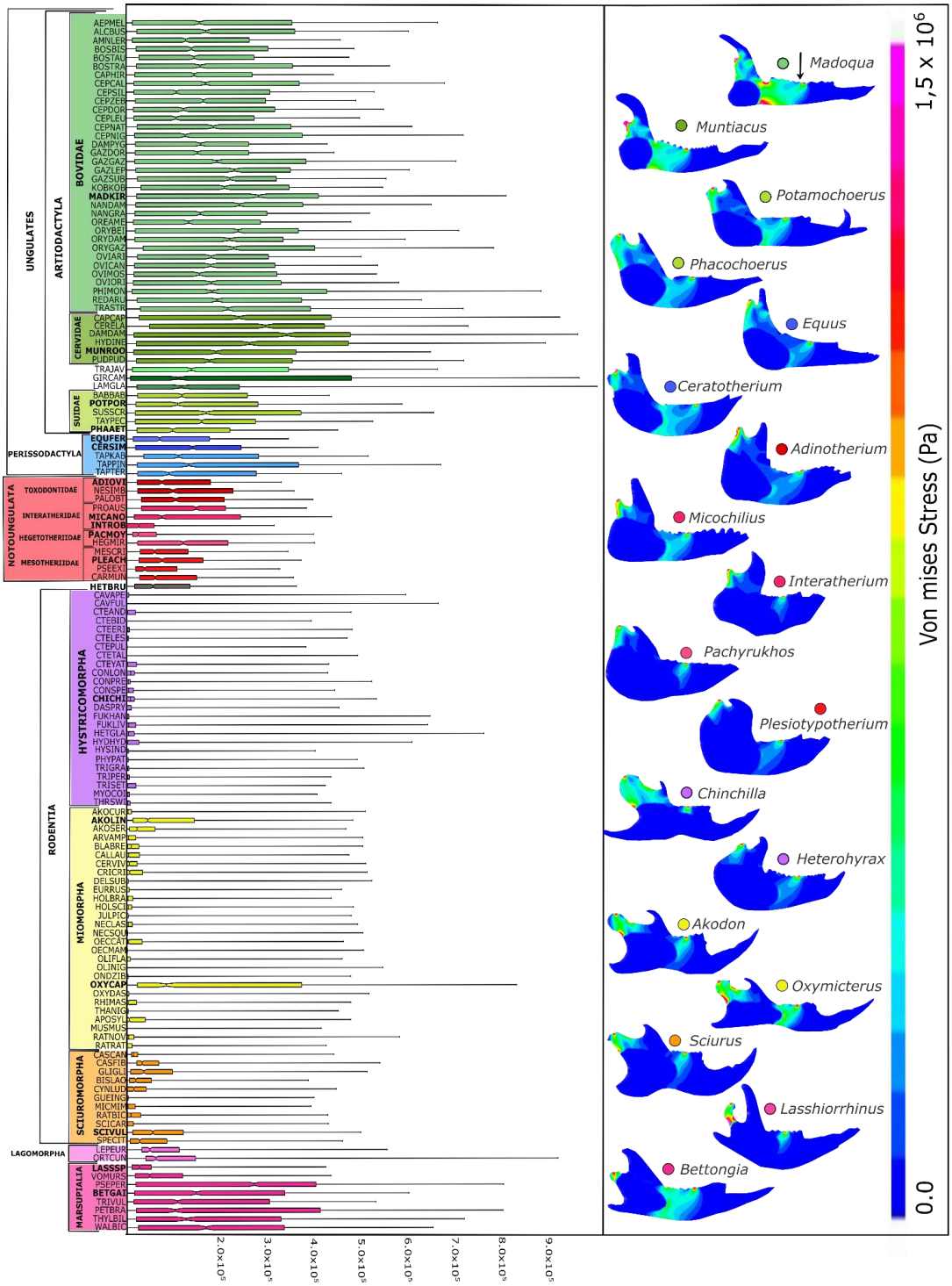


Fig. 5. Finite element analysis results for BP1. Left: boxplots of von Mises stress for each taxon; an asterisk indicates mean stress <1 MPa. Right: selected 2D mandible–tooth FEA results with the corresponding von Mises stress scale on the far-right y-axis. Bold letters on the left and coloured circles on the right indicate corresponding specimens. Species abbreviations are provided in Supplementary Table S1 online.



744

745 **Fig. 6.** Finite element analysis results for BP4. Left: boxplots of von Mises stress for each taxon; an asterisk
746 indicates mean stress <1 MPa. Right: selected 2D mandible–tooth FEA results with the corresponding von Mises
747 stress scale on the far-right y-axis. Bold letters on the left and coloured circles on the right indicate corresponding
748 specimens. Species abbreviations are provided in Supplementary Table S1 online.

749

Supplementary Files

This is a list of supplementary files associated with this preprint. Click to download.

- SupplementaryArriagadaetal.Scientificreports.docx